Photon acceleration of ultrashort laser pulses by relativistic ionization fronts

J. M. Dias, N. C. Lopes, L. O. Silva, G. Figueira, and J. T. Mendonça
GoLP/Centro de Física de Plasmas, Instituto Superior Técnico, 1049-001 Lisboa, Portugal

C. Stenz,[1,2] F. Blasco,[1,2] A. Dos Santos,[1] A. Mysyrowicz[1]
[1]*LOA, ENSTA/cole Polytechnique-CNRS, 91120 Palaiseau, France*
[2]*Centre Lasers Intenses et Applications, Universit Bordeaux 1, 33405 Talence, France*
(Received 27 July 2001; revised manuscript received 2 August 2002; published 15 November 2002)

We present experimental results from the collision of weak ultrashort pulses with relativistic ionization fronts in copropagation and counterpropagation. The observed frequency upshifts of the probe pulses provide not only information about the electron density of the ionization front but also reveal the fine structure of the front. The connection between the correlation lengths for copropagation and counterpropagation and the longitudinal and transverse dimensions of the ionization front is also demonstrated thus showing the feasibility of using the frequency upshift experienced by short probe pulses to fully characterize relativistic ionization fronts and other relativistic coherent structures in laser-produced plasmas.

DOI: 10.1103/PhysRevE.66.056406 PACS number(s): 52.38.−r, 52.59.−f, 52.70.Kz

I. INTRODUCTION

The designation *photon acceleration* was coined by Wilks *et al.* [1], to describe the combined effect of frequency upshift with photon number conservation experienced by a probe laser pulse copropagating in a relativistic electron plasma wave. Strong tunable frequency upshifts can also be obtained whenever electromagnetic waves interact with relativistic ionization fronts [2–6]: even though the classical number of photons is not conserved here, the term photon acceleration has also been widely used to describe this scenario. The possibility to control, to tune, and to accurately measure the frequency upshift of short laser pulses interacting with ionization fronts and relativistic plasma waves has triggered considerable work in this subject, in connection with tunable radiation sources [7] and laser wakefield diagnostics from plasma based accelerators [8–10].

An intense short laser pulse propagating through a gas can generate a relativistic front by optical-field induced ionization of the background gas. The ionization front propagates with approximately the group velocity of the ionizing laser pulse in the interface gasplasma, and the rise time is roughly half the laser pulse duration, while the maximum electron density of the front is a function of the background gas pressure and the laser intensity. The electron density behind the front evolves in a longer time scale, the recombination time scale ($\sim \mu s$). A short weak laser pulse colliding with an ionization front can be double Doppler upshifted by the front, for reflection. Even when the front is not dense enough for total reflection, and the probe pulse is transmitted across the front, the frequency shift can be significant [5,6,11].

Theoretical work on this problem has been based on plane wave analysis [2,3,5], eigenmode expansion in a cavity [12], the ray-tracing or Hamiltonian formulation [6,11], and photon kinetics [13]. The first two approaches are a natural description for microwave beams, and ray tracing and photon kinetics seem to be the suitable formalisms for short pulses. The ray-tracing equations are only valid in the geometrical optical approximation, i.e., the time scale τ_p (length scale) of the perturbation is much longer than the period (wavelength, λ) of the wave packet $2\pi/\omega \ll \tau_p$, which means that $\lambda[\mu\mathrm{m}] \ll 0.3\tau_p[\mathrm{fs}]$. These conditions are usually satisfied when probing is performed by a low intensity, short pulse, with a central frequency much higher than the electron plasma frequency.

The key feature predicted by the theory is the significant difference between the frequency upshift $\Delta\omega$ for counter and copropagation [6], i.e.,

$$\Delta\omega = \frac{\omega_{pe0}^2}{2\omega_0}\frac{\beta_f}{1\pm\beta_f}, \tag{1}$$

for a one-dimensional (1D) configuration in a underdense ionization front, where the plus(minus) sign pertains to counter(co)propagation, and $\omega_{pe0}=(4\pi n_{e0}/m_e)^{1/2}$ is the maximum electron plasma frequency of the front, ω_0 is the initial frequency of the probe pulse, and β_f is the velocity of the front, normalized to the speed of light c.

However, and in reality, 2D scenarios are more plausible and finite width ionization front effects can be important [14]. To address these conditions it is necessary to solve numerically the ray-tracing equations [6,14]:

$$\dot{\mathbf{k}} = \frac{d\mathbf{k}}{dt} = -\frac{\partial\Omega}{\partial\mathbf{x}} = -\frac{1}{2\Omega}\frac{\partial\omega_{pe}^2}{\partial\mathbf{x}}, \tag{2}$$

$$\dot{\mathbf{x}} = \frac{d\mathbf{x}}{dt} = \frac{\partial\Omega}{\partial\mathbf{k}} = \frac{\mathbf{k}c^2}{\Omega}, \tag{3}$$

$$\dot{\Omega} = \frac{d\Omega}{dt} = \frac{\partial\Omega}{\partial t} = \frac{1}{2\Omega}\frac{\partial\omega_{pe}^2}{\partial t}, \tag{4}$$

in order to simulate those configurations, with $\Omega=[\mathbf{k}^2c^2+\omega_{pe}^2(\mathbf{x},t)]^{1/2}$, the local frequency from the linear dispersion relation, playing the role of the Hamiltonian, and $\mathbf{k}$ and $\mathbf{x}$ are the canonical momentum, or wave vector, and canonical position, respectively, and $\omega_{pe}^2(\mathbf{x},t)=4\pi e^2 n_e(\mathbf{x},t)/m_e$ is the local electron plasma frequency squared, where $n_e(\mathbf{x},t)$ is

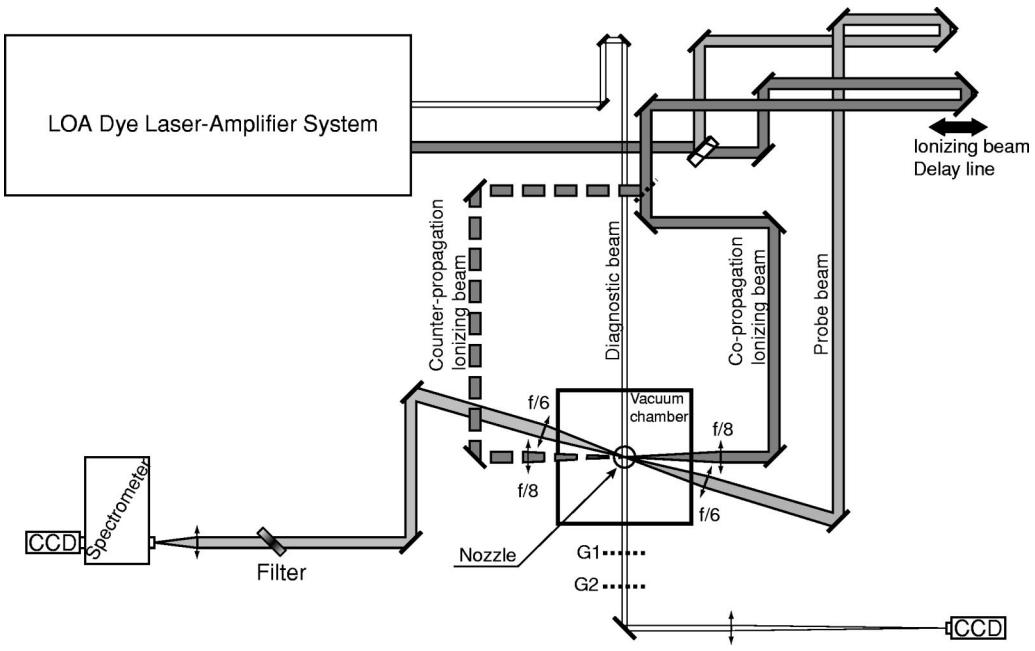

FIG. 1. Experimental setup.

the local electron density of the ionization front, m_e is the electron mass, and e is the electron charge.

The frequency upshift of laser pulses in plasmas has been verified experimentally in different configurations [15–18]. However, these results could not distinguish between the frequency upshift due to a relativistic ionization front or the frequency upshift due to an almost instantaneous and uniform local increase of the electron density, or flash ionization. In fact, significant upshift have been observed at a tight focus of the ionizing beam [19]. When this sudden growth of plasma occurs and the plasma changes only in time $n_e(t)$, in a few cycles of the electromagnetic radiation, the ray tracing theory is no longer valid and the phase effects became dominant. Since frequency upshifts by flash ionization are associated with homogenous plasma growth in time, the flash ionization frequency upshift does not depend on the collision angle, and can be obtained from Eq. (1) when $\beta_f \rightarrow \infty$:

$$\Delta\omega \approx \frac{\omega_{pe0}^2}{2\omega_0}. \tag{5}$$

In order to clearly separate the two frequency upshift regimes, photon acceleration and flash ionization, it is necessary to compare the frequency upshift obtained for two different collision angles [19]: only then we will be able to clearly identify the presence of a relativistic ionization front.

In this paper, we present detailed experimental results of photon acceleration by relativistic ionization fronts, recently reported elsewhere [19]. By comparing the frequency upshift experienced by a short laser pulse for two distinct incidence angles on the front, we are able to clearly show that a relativistic ionization front is responsible for the upshift we also determine the fundamental characteristics of the front i.e. its velocity β_f, and maximum electron density n_{e0}. Furthermore, a two-dimensional (2D) configuration has been adopted thus allowing for the illustration of some of the peculiarities predicted by the theory of photon acceleration by ionization fronts in 2D [14].

This paper is organized as follows. First, we describe the experimental set-up, and we identify the different configurations employed in the experiment. The experimental results are presented and discussed in Sec. III, along with comparisons with two-dimensional ray-tracing simulations. Finally, in the last section, the conclusions are stated.

II. EXPERIMENTAL SETUP

In the two-dimensional collision of a probe short laser pulse with a relativistic ionization front, we have employed the experimental scheme shown in Fig. 1. This experiment makes use of a dye laser-amplifier system at LOA (Laboratoire d'Optique Appliquée). The main laser specification consists of nearly transform-limited pulses with a pulse duration of 80 fs at the oscillator output and an energy of 5 mJ at the end of the laser chain. The central wavelength is $\lambda = 620$ nm and the repetition rate is 10 Hz.

The ionization front is produced by focusing about 50% ($\sim$2.5 mJ) of the main laser beam (ionizing laser beam), with an f/8 achromat (25 cm of focal length) in a gas jet. The peak vacuum intensity of $\sim 7\times10^{15}$ W/cm^2 is obtained for a focal spot of 14 μm in radius. The focal point is located at the border of the vacuum surrounded gas jet in order to obtain maximum plasma density. If focused at the central zone of the jet, where the neutral density is higher, the produced plasma would defocus the ionizing beam before reaching the focal point, contributing for a much lower plasma density [20]. We have employed a supersonic argon jet, in a pulsed regime with high pressure (70 mbar) at the nozzle, capable of producing high density flows of 2×10^{19} cm^{-3} at the flattop center, and 10^{19} cm^{-3} at the border, where the collision with the probe pulse occurs [21].

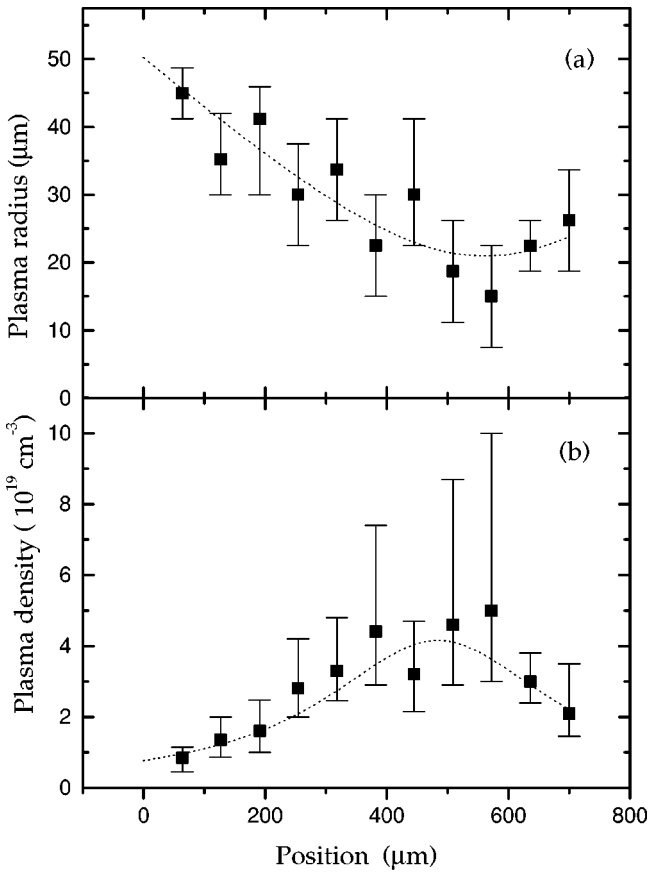

FIG. 2. (a) Plasma radius and (b) electron plasma density, as a function of the position along the laser propagation axis, measured by Moiré interferometry.

The photons to be frequency upshifted (probe laser beam) correspond to a small fraction (0.05%) of the ionizing beam, with an energy around 1 μJ. The signal to noise ratio in the blue shifted signal is also increased by focusing the probe beam in the region of ionization front formation (which is the focal region of the ionizing beam) by using an f/6 achromat (20 cm focal length) producing a focal spot of $\sim 11\ \mu$m, corresponding toa focused intensity of 4×10^{12} W/cm^2. This low intensity was necessary in order to guarantee that the probe beam does not ionize the background gas. After the collision of the probe pulse with the ionization front, the probe photons are collected by an f/6 lens and sent to the spectrometer.

An angle of 20° between the ionization front and the probe pulse, allowed us to decouple the observation of the blue shift of the probe photons to the expected self-blueshift of the ionizing beam, and also to examine the two-dimensional features of the relativistic collision. In performing our experiments, the probe laser beam was kept in a fixed position. Copropagation and counterpropagation of this beam with respect to the ionization front was then obtained by changing the direction of the ionization front (or the propagation direction of the ionizing laser beam) (see Fig. 1). The plasma density gradients lead to significant refraction effects, mainly if the probe pulse collides mostly with the preformed plasma left behind the ionization front, which was clearly observed during the experiment. In order to check the sensitivity of the measurements in the spectrometer to this refraction effects, a Dove prism was used, and a diffuser was placed at the spectrometer entry slit. For low efficiency measurements in the copropagation configuration, we used a filtering mirror (see Fig. 1) to cut radiation above 600 nm, in order to minimize the unshifted radiation ($\approx$620 nm). Those spectra were then corrected by the filter calibration curve.

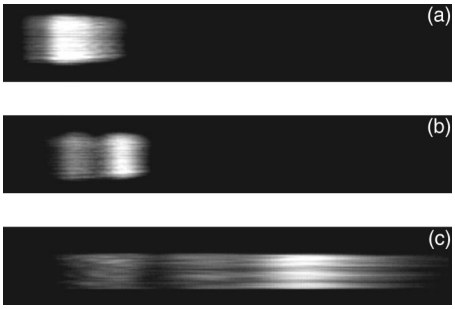

FIG. 3. Typical CCD images from the spectrograph of the probe: (a) without the presence of a plasma; (b) after the interaction with a counterpropagating ionization front; (c) after the interaction with a copropagating ionization front.

A third laser beam, for diagnostics, with a duration of 35 fs, central wavelength of $\lambda = 560$ nm at a repetition rate of 10 Hz is also produced by the laser system with an energy of a few μJ. This beam is created also from the same dye laser chain, so the main laser pulse and the diagnostic laser pulse were always synchronized since they have the same origin. With this third beam, we have measured the electron plasma density associated with the ionization front by using a Moiré interferometer represented in Fig. 1 by the two grids G_1 and G_2. By using the Moiré interferometry technique [21], it is possible to determine the electron plasma density and the transverse width of the ionization front. In Fig. 2 we present a typical plasma density profile along the laser axis and the ionization front radius. By removing the grids it is also possible, using the same system, to observe the formation and displacement of the ionization front produced by the ionizing laser beam, employing a shadowgraphic technique.

The probe pulse spectra (Fig. 3) consisting of two CCD images of the spectrograph (before and after collision with the front) are vertically integrated, in order to obtain the power spectrum of the probe beam before and after the interaction with the ionization front.

Typical power spectra of the probe beam are shown in Fig. 4. To determine the frequency upshifts, an automatic multi-Gaussian fit was performed on the spectra, thus providing the peak frequency/wavelength for each gaussian, and thus giving us the frequency shift due to the collision with the ionization front, Fig. 4. A Gaussian fit was used because the frequency upshift mechanisms are adiabatic and nonresonant which means that all the signal is transferred from one region of the spectrum to another, without any selection rule and maintaining the same approximate spectral shape. The peak intensities are also obtained from this fitting procedure.

III. EXPERIMENTAL RESULTS

During the experiment we were able to introduce two types of variations with the aim of changing some of the ionization front parameters, and interaction features.

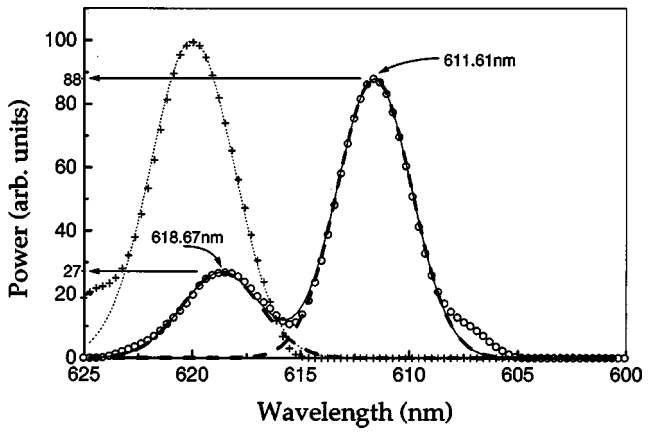

FIG. 4. Typical power spectra of the probe pulse in the spectrometer. The dotted Gaussian curve represents the unshifted probe signal by fitting several points of the spectral data (plus signs) of the probe pulse without interacting with the plasma. The open circles are the upshifted spectrum data, after the collision with the ionization front, used to performed a multi-Gaussian fit (solid curve). The Gaussian dashed curves represent each upshifted frequency peak separately obtained from the multi-Gaussian fitting process.

A. Local plasma density and the fine structure of the ionization front

In order to vary the plasma density of the front we moved longitudinally the achromat in the optical circuit of the ionizing beam (see Fig. 5). The plasma density variation was associated with a change of the ionizing beam diameter and intensity at the interaction region between the two beams. The interaction region was kept fixed, as shown in Fig. 5.

The critical issue when analyzing frequency upshift by ionization fronts is the comparison between copropagation and counterpropagation. In Fig. 6, we plot the frequency upshifts as a function of the focusing lens (achromat) position in copropagation and in counterpropagation scenarios: each peak in the spectrum contributes with a point assigned by the underlying upshift mechanism.

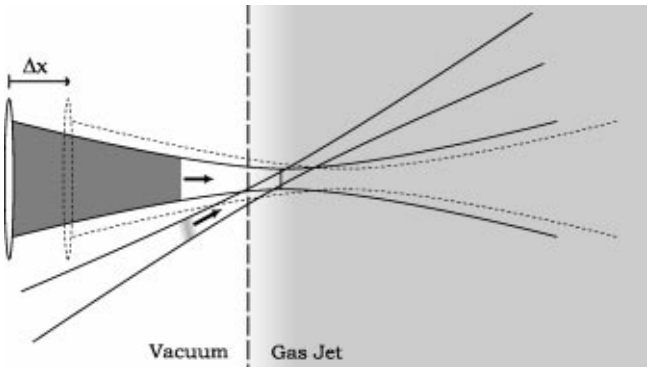

FIG. 5. Sketch illustrating the plasma density variation by moving longitudinally the focusing lens position of the ionizing beam. The achormat focus the ionizing pulse in border region of the gas jet where the probe is also focused with an angle of 20 degrees. The dashed lines indicate the new ionizing beam profile at the collision region after displacing the focusing achormatic lens by Δx.

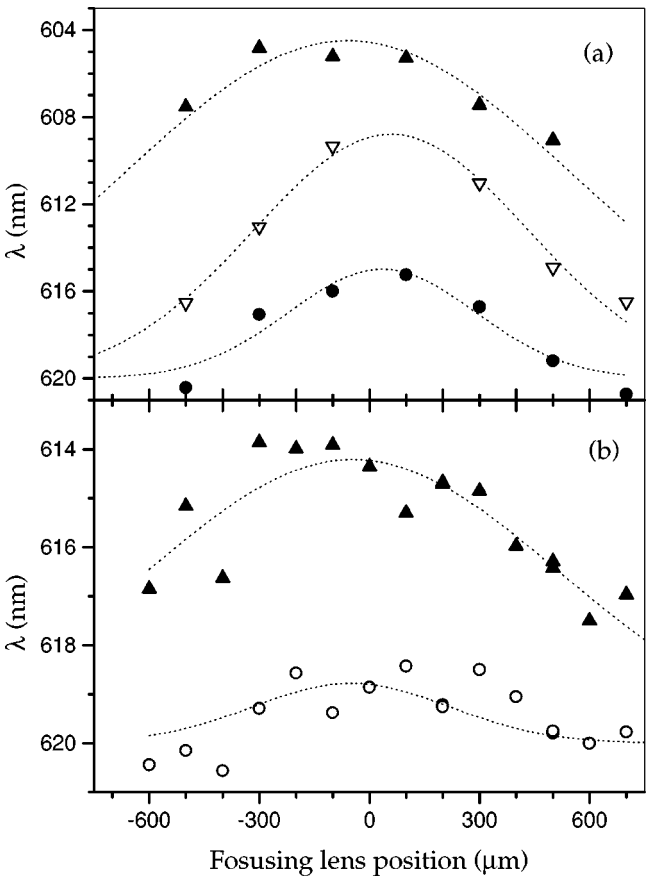

FIG. 6. Frequency upshift as function of the focusing lens position of ionizing beam. (a) in copropagation: (solid uptriangles) photon acceleration; (open downtriangles) intermediate frequency upshift; (solid circles) flash ionization. (b) in counterpropagation: (solid uptriangles) due to the photon acceleration, (open circles) due to flash ionization. The dashed curves are Gaussian fits to give a visual aid of the variation.

The maximum upshift attained is $\Delta\lambda_{max}=15.6$ nm in Fig. 6(a) for the copropagation which clearly correspond to a photon acceleration effect in the ionization front with a plasma density of 4.5×10^{19} cm^{-3} given by ray-tracing simulations [19,14]. The curve with lower-frequency upshift are in very good agreement with the expected value of the flash ionization effect for those plasmas densities of the ionization front on both cases $\Delta\lambda_{max}=4.75$ nm for $n_e=4.5\times10^{19}$ cm^{-3} [Fig. 6(a)] calculated from Eq. (5). On the other hand, for the counter-propagation [Fig. 6(b)], we to identify the curve with higher upshifts (with a maximum of around the 5.5 nm) as flash ionization phenomena, because the predicted plasma density of the ionization front to reach this upshift by photon acceleration would be of the order of 10^{20} cm^{-3}, which clearly is out of range for our experimental setup. From Eq. (5) we can then determine the electron density $n_e=5.2\times10^{19}$ cm^{-3} to obtain this frequency upshift. The blue shift due to the photon acceleration (curve with lower-frequency upshifts) only reaches a little more than 1.5 nm which corresponds to a ionization front with a plasma density around $3.0\times10^{1}9$ cm^{-3} given by ray-tracing simulations [19,14]. Comparing the plasma density results ob-

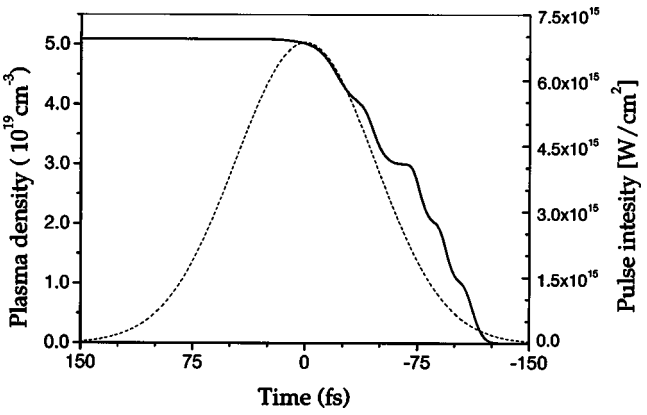

FIG. 7. Predicted shape ionization front by the ionizing pulse from the multiphoton and tunneling ionization theory. The dashed curve represents the laser pulse and the solid line the generated plasma density of the ionization front at the beam axes.

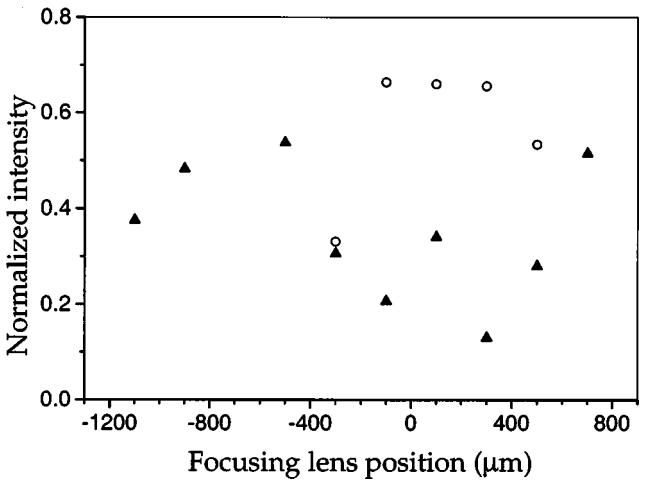

FIG. 8. Peak intensities of the observed spectra as function of the focusing lens position of ionizing beam in copropagation. (Solid uptriangles) sum of the maximum with the intermediate frequency upshifts peak intensities related to the photon acceleration phenomena; (open circles) peak intensity associated to the flash ionization.

tained from the frequency upshift in both scenarios, we can confirm that the maximum plasma density of the ionization front (between 4.5 and 5.0×10^{19} cm^{-3}) was similar for these two configurations. This density estimate also agrees with the measurements from the Moiré interferometry.

Also from Fig. 6(a), it is clear that there is a third curve between the two mentioned frequency shifts. This intermediate shift has a maximum of 10 nm in wavelength which would correspond of a plasma density of around 3.0×10^{19} cm^{-3}, from the ray-tracing simulations [19,14] of the photon acceleration phenomena. This is not a flash ionization effect because this upshift would correspond to a density of approximately 10^{20} cm^{-3}, which is not compatible with our laser and gas jet parameters.

A plausible explanation for this intermediate upshift is given by the ionization steps of the Argon at the ionization front. In Fig. 7 we can see the predicted shape of a ionization front obtained by the ionization theory applicable to these gas conditions and laser intensity [22–24], using the data from the multiphoton and tunneling ionization experiments of noble gases [25–27]. In the ionization of the Argon there is a considerable time lag between the ionization of Ar^{3+} and the ionization of Ar^{4+}. Thus, a significant fraction of photons from the probe pulse interact only with the outer zone of the ionization front, that only reaches the third level of the ionization. We have confirmed this with ray-tracing simulations. Those photons will give rise to the intermediate frequency upshift, which is sufficiently efficient to be discriminated in probe beam spectrum.

In counterpropagation [Fig. 6(b)] the frequency upshifts are smaller than the probe pulse spectral width and so it is very difficult to distinguish all the different frequency upshifted peaks due to the spectral overlapping. Nevertheless, the maximum density associated to the photon acceleration upshift is given by the third level of ionization of Argon (Ar^{3+}) and can be explained by the same arguments mentioned for the copropagation results.

In order to corroborate the presence of flash ionization it is important to study the relative importance of between the two upshift mechanisms, photon acceleration and flash ionization in different collision regions. From the evolution of the normalized peak intensities in the probe beam spectrum for copropagation collisions, Fig. 8, it is possible to observe the competition, between the two mechanisms, near or away the focal region of the ionizing beam. We see that photon acceleration and flash ionization dominate in different zones of the collision of the probe pulse with ionization front. In the first case it is clear that the signal due to flash ionization is dominant in the focal zone of the ionizing beam, where the plasma density is higher but the ionization front is smaller (~20 μm from the Moiré interferometry) and less well defined. In small spot size focal region, the probe experiences a uniform increase of the plasma density along its full extent: this is the flash ionization scenario. We stress that a similar behavior is observed in counterpropagation.

B. Ionization front characterization

In order to retrieve the features of the ionization front we have studied the influence of the delay between the ionizing pulse and the probe pulse in the frequency upshift data results. This was achieved by varying the delay line at the ionizing beam optical circuit (see Fig. 1). By changing this delay the interaction zone was no longer kept fixed, since the interaction between the ionization front and the probe pulse depends on the time and space overlap of the two pulses (see Fig. 9). In the copropagation configuration there is essentially a time overlap (or cross-correlation) between the ionization front and the probe pulse. For counterpropagation, the collision between the laser pulses (probe and ionizing) occurred at different positions of their trajectories, so the interaction is limited by the space overlap of the two beams at the gas jet.

This can give us the length along the beam trajectory where the probe pulse experience the frequency upshift. We can call this a correlation length (delay time $\times$ light speed), and measure it for the two experimental configurations (copropagation and counterpropagation). In copropagation we have a cross correlation in time between the ionization front

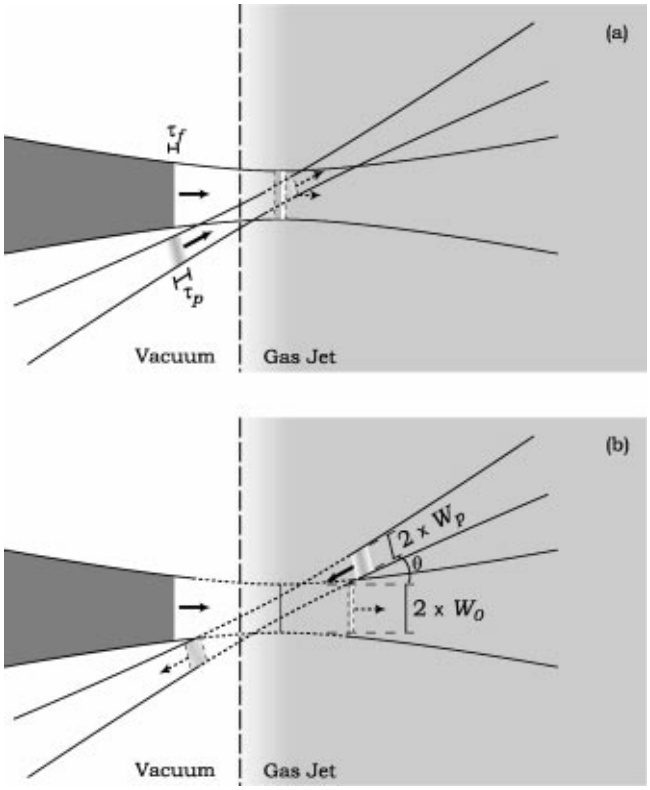

FIG. 9. Schematic illustration of interaction zone (a) in copropagation and (b) in counterpropagation when varying the delay line at the ionizing beam optical circuit. The dashed lines indicate, in both cases, the correlation length in the trajectories where the collision between the ionization front and the probe pulse can occur. τ_f and τ_p are the ionization front duration and the probe pulse duration, respectively. $2\times W_0$ and $2\times W_p$ are the ionizing beam (i.e., ionization front) and the probe beam diameters, respectively.

and the probe pulse; therefore, the interaction length D_{co} is a function of the probe pulse duration, τ_p, and the ionization front duration τ_f ($\approx$ half of the ionizing pulse duration) given by the approximate relation:

$$D_{co} \approx c(\tau_f + \tau_p). \tag{6}$$

On the other hand, in counterpropagation the interaction length corresponds to the region where the trajectory of the ionization front overlaps the trajectory of the probe pulse. In this case the correlation length, $D_{counter}$, is determined by

$$D_{counter} \approx \frac{2(W_0 + W_p)}{\theta}, \tag{7}$$

where W_0 and W_p are the ionization front and probe beam radius, respectively and θ is the angle between the two trajectories.

The correlation length in co-propagation is around 60 μm (width at half maximum and 100 μm in total), see Fig. 10, which would correspond to an ionization front rise time of 65 fs, which implies that the laser pulse duration should be around 2×65 fs$=130$ fs.

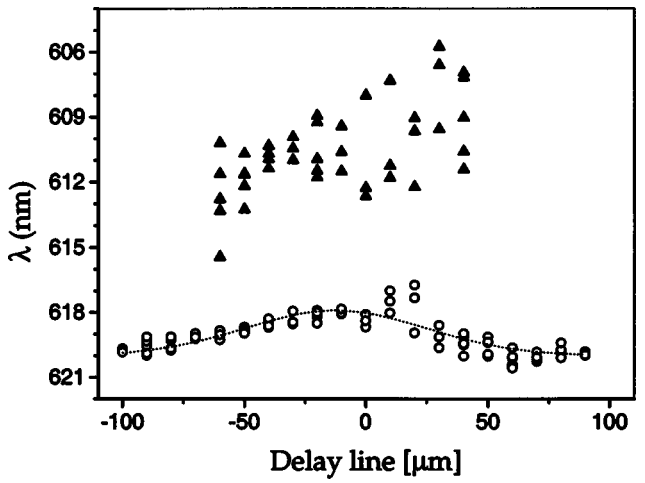

FIG. 10. Frequency upshift as function of the delay line in the ionizing beam path for copropagation: (solid uptriangles) due to photon acceleration; (open circles) frequency upshift associated to the flash ionization.

This pulse duration is a slightly larger than the laser specifications, but it is consistent with the measured probe pulse spectra.

The correlation length in counterpropagation is of the order of 2×135 μm (width at half maximum), see Fig. 11. Considering that $W_p = 0.8W_0$, due to the focal length relation of the lens used for the ionizing and probe beams and an angle θ between them of 20 degrees, we retrieve the ionization front width $\approx 2\times W_0 = 26.5$ μm, which agrees well with the results obtained by Moiré interferometry [see Fig. 2(a)].

By confirming the time and space dimensions of the ionization front, these results clearly demonstrate the ability to determine the dimensions of the ionization front (duration and width) from the correlation lengths observed in the two experimental configurations.

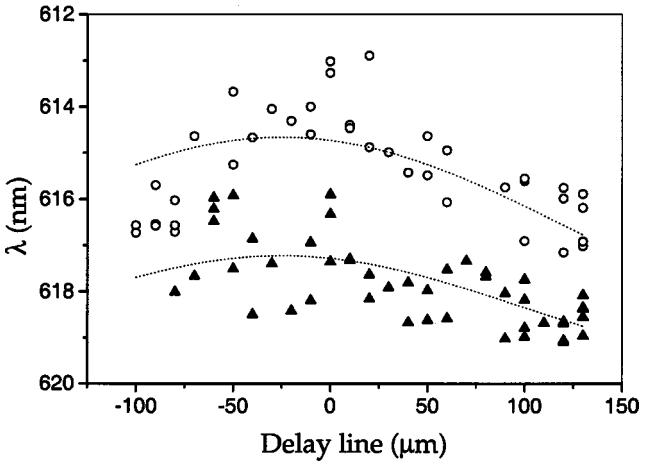

FIG. 11. Observed frequency upshift as function of the delay line in the ionizing beam path for counterpropagation. (Solid uptriangles) measured frequency upshift related to the photon acceleration phenomena; (open circles) frequency upshift associated to the flash ionization. The dashed curves are Gaussian fits to give a visual aid of the variation and the correlation length ($\sim 2\times 135$ μm width at half maximum).

IV. CONCLUSIONS

We have presented a 2D experimental setup for studying the frequency upshift suffered by a probe laser pulse in the interaction with a relativistic ionization front. The retrieved plasma densities associated with observed maximum frequency shifts are in good agreement with the measurements from Moiré interferometry. This agreement is also present when comparing the results from the co-propagation and counter-propagation experimental configurations.

The experimental results also show evidence for a contribution to the power spectra of a signal that has approximately the same frequency upshift in the copropagation configuration as in the counter-propagation case. We interpret this as a clear signature of the well-known flash ionization effect. From the intensity plots in copropagation and counterpropagation, we confirm that the photon acceleration signal is more efficient before the focus position, where the ionization front is larger and well defined. On the contrary, near the focus flash ionization becomes dominant. In those cases the incident probe photons no more experience the influence of a well-defined front, but they sample the entire plasma region, which is suddenly being generated.

With our 2D experimental setup we were able to demonstrate that it is possible to retrieve several characteristics of the ionization front by measuring frequency upshifts induced by photon acceleration. When varying the focusing lens position of the ionizing beam the observation of intermediate frequency upshifts due to ionization steps of the Argon, clearly shows the ability to probe the fine structure of the ionization front by photon acceleration. On the other hand, the correlation lengths obtained by varying the time delay between the probe and the ionizing pulses, determines the overlap of the two pulses in time and in space, thus enabling us to determine the time duration and transversal dimension of the front, from the copropagation and counterpropagation datas, respectively. Those results were confirmed by the Moiré interferometry measurements and the pulse duration estimate from the spectral width of the probe laser pulse before entering the plasma. Our results demonstrate the viability of frequency upshift measurements by weak probe pulses as a powerful diagnostic tool for relativistic coherent structures in laser-produced plasmas.

ACKNOWLEDGMENT

This work was partially supported by FCT (Portugal).

[1] S.C. Wilks *et al.*, Phys. Rev. Lett. **62**, 2600 (1989).
[2] M. Lampe, E. Ott, and J.H. Walker, Phys. Fluids **10**, 42 (1978).
[3] V.I. Semenova, Sov. J. Radiophys. Quantum Electron. **10**, 599 (1967).
[4] J.T. Mendonça, J. Plasma Phys. **22**, 15 (1979).
[5] W.B. Mori, Phys. Rev. A **44**, 5118 (1991).
[6] J.T. Mendonça and L.O. Silva, Phys. Rev. E **49**, 3520 (1994).
[7] J.R.L. Savage, C. Joshi, and W.B. Mori, Phys. Rev. Lett. **68**, 946 (1992).
[8] J.R. Marquès *et al.*, Phys. Rev. Lett. **76**, 3566 (1996).
[9] C.W. Siders *et al.*, Phys. Rev. Lett. **76**, 3570 (1996).
[10] J.M. Dias, L.O. Silva, and J.T. Mendonça, Phys. Rev. ST Accel. Beams **1**, 031301 (1998).
[11] L.O. Silva and J.T. Mendonça, IEEE Trans. Plasma Sci. **24**, 316 (1996).
[12] L.O. Silva and J.T. Mendonça, IEEE Trans. Plasma Sci. **24**, 503 (1996).
[13] L.O. Silva and J.T. Mendonça, Phys. Rev. E **57**, 3423 (1998).
[14] J.M. Dias *et al.*, Phys. Rev. E **65**, 036404 (2002).
[15] N. Bloembergen, Opt. Commun. **8**, 285 (1973).
[16] E. Yablonovitch, Phys. Rev. Lett. **31**, 877 (1973).
[17] S.C. Rae and K. Burnett, Phys. Rev. A **46**, 1084 (1992).
[18] S.C. Wilks, J.M. Dawson, and W.B. Mori, Phys. Rev. Lett. **61**, 337 (1988).
[19] J.M. Dias *et al.*, Phys. Rev. Lett. **78**, 4773 (1997).
[20] C. Stenz, K. Ekbom, F. Blasco, and J. Stevefelt, Rapport LULI, 7 (1996).
[21] C. Stenz, R. Brückner, F. Blasco, and J.C. Pellicer, Rapport LULI, 326 (1993).
[22] L.V. Keldysh, Zh. Eksp. Teor. Fiz. **47**, 1945 (1964) [Sov. Phys. JETP **20**, 1307 (1965)].
[23] M.V. Ammosov, N.B. Delone, and V.P. Kraĭnov, Zh. Eksp. Teor. Fiz. **91**, 2008 (1986) [Sov. Phys. JETP **64**, 1191 (1986)].
[24] B.M. Penetrante and J.N. Bardsley, Phys. Rev. A **43**, 3100 (1991).
[25] M.D. Perry, O.L. Landen, A. Szöke, and E.M. Campbell, Phys. Rev. A **37**, 747 (1988).
[26] S. Augst *et al.*, Phys. Rev. Lett. **63**, 2212 (1989).
[27] S. Augst, D.D. Meyerhofer, D. Strickland, and S.L. Chin, Phys. Rev. Lett. **8**, 858 (1991).